Science of the Total Environment 599–600 (2017) 944–951

Contents lists available at ScienceDirect

Science of the Total Environment

journal homepage: www.elsevier.com/locate/scitotenv

Modeling carbon emissions from urban traffic system using mobile monitoring

Daniel (Jian) Sun [a,b,c,*], Ying Zhang [c], Rui Xue [d], Yi Zhang [b,e]

[a] State Key Laboratory of Ocean Engineering, Shanghai Jiao Tong University, Shanghai 200240, China
[b] China Institute of Urban Governance, Shanghai Jiao Tong University, Shanghai 200240, China
[c] Center for ITS and UAV Applications Research, Shanghai Jiao Tong University, Shanghai 200240, China
[d] Fuzhou Planning & Design Research Institute, Fuzhou 350108, China
[e] Sustainable Residential Environment Research Center, Shanghai Jiao Tong University, Shanghai 200240, China

HIGHLIGHTS

- Constructed an urban carbon emission monitoring system using **mobile monitors** and collected traffic characteristics and meteorological data.
- Identified the traffic carbon emission at **microscopic, mesoscopic and macroscopic levels, and assessed t**he major influenced factors.
- VSP-bin is categorized into: **idle, low velocity, medium velocity and high velocity**, so as to figure out the proportion of idling condition for MOVES.
- With the final carbon emission factors calculated by MOVES, **arterial traffic** was identified to generate the major carbon emissions among the urban road system.

GRAPHICAL ABSTRACT

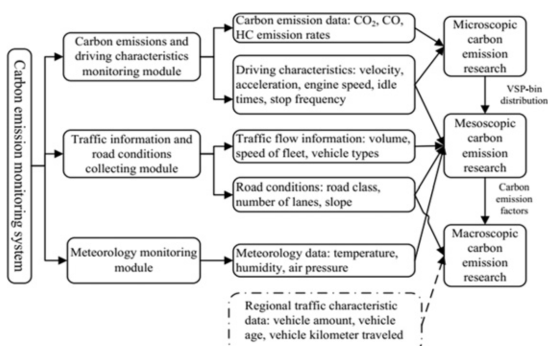

ARTICLE INFO

Article history:
Received 28 March 2017
Received in revised form 24 April 2017
Accepted 25 April 2017
Available online 11 May 2017

Editor: D. Barcelo

Keywords:
Urban traffic
Carbon emissions
Mobile monitoring
MOVES
Emission factor

ABSTRACT

Comprehensive analyses of urban traffic carbon emissions are critical in achieving low-carbon transportation. This paper started from the architecture design of a carbon emission mobile monitoring system using multiple sets of equipment and collected the corresponding data about traffic flow, meteorological conditions, vehicular carbon emissions and driving characteristics on typical roads in Shanghai and Wuxi, Jiangsu province. Based on these data, the emission model MOVES was calibrated and used with various sensitivity and correlation evaluation indices to analyze the traffic carbon emissions at microscopic, mesoscopic and macroscopic levels, respectively. The major factors that influence urban traffic carbon emissions were investigated, so that emission factors of CO, CO_2 and HC were calculated by taking representative passenger cars as a case study. As a result, the urban traffic carbon emissions were assessed quantitatively, and the total amounts of CO, CO_2 and HC emission from passenger cars in Shanghai were estimated as 76.95 kt, 8271.91 kt, and 2.13 kt, respectively. Arterial roads were found as the primary line source, accounting for 50.49% carbon emissions. In additional to the overall major factors identified, the mobile monitoring system and carbon emission quantification method proposed in this study are of rather guiding significance for the further urban low-carbon transportation development.

* Corresponding author.
E-mail addresses: danielsun@sjtu.edu.cn (D.(J.) Sun), haipingxian@sjtu.edu.cn (Y. Zhang), xueruijerry@sjtu.edu.cn (R. Xue), darrenzhy@sjtu.edu.cn (Y. Zhang).

http://dx.doi.org/10.1016/j.scitotenv.2017.04.186
0048-9697/

1. Introduction

The rapid urbanization, motorization, and economic growth in China over the past ten years have resulted in severe environmental deterioration, in particular, the sharp growth of traffic emissions. World Energy Outlook predicted that urban traffic-related carbon emission would increase at an annual rate of 1.7% from 2010 to 2030, while the annual growth rates of traffic-related carbon emissions in developing countries and moderately developed countries, are projected at 3.4% and 4.2%, respectively (Aleklett et al., 2010). When it comes to Shanghai, mobile source emissions are responsible for approximately 78% of carbon monoxide (CO) and 83% of hydrocarbons (HC) according to the statistics (Wang et al., 2008a). To attain an international climate change agreement at Copenhagen or beyond, the Chinese government announced the long-term pledge to reduce carbon emissions by 40–45% by 2020 relative to the standard in 2005 (Zhang, 2011). To achieve this ambitious goal, understanding traffic-related carbon emissions at different spatial and temporal scales is essential, so that to stipulate effective policies and strategies for carbon emission management. To this end, comprehensive investigations utilizing efficient tools and data sources are crucial to avoid high uncertainties or mistakes brought by assumptions or roughly qualitative intuitions.

During the carbon emission monitoring, conventional studies generally relied on engine dynamometer testing and remote sensing (Franco et al., 2013), in which the emission rates were measured by simulating driving cycle. Pelkmans and Debal (2006) used new European driving cycle (NEDC) to measure CO, CO_2, HC emissions of various light-duty gasoline vehicles in engine dynamometer, revealing the connection between emissions and driving characteristics. However, the measurement generally takes longer duration and is not consistent with real-world driving conditions (Smit et al., 2010). On the contrary, the on-road remote sensing system which generally has comparative high sampling rate and rapid detecting speed has been used in many cities, such as Los Angeles and Mexico City (Burns et al., 2012). Guo et al. (2007a,b) used the remote sensing equipment to collect both emissions and driving characteristics of real-world vehicle fleet, and generated travel-based emission inventories for Hangzhou, China. Nevertheless, the remote sensing system doesn't work appropriately while monitoring heavy-polluting vehicles and the non-uniform height of tailpipes may also introduce errors. Consequently, portable emissions measurement systems (PEMS) for onboard measurement of exhaust emissions were introduced (Liu et al., 2009). Second-by-second data from PEMS allow quantifying the representative cycles and corresponding emissions (DeFries et al., 2014), which are useful in developing emission inventories for a wide range of vehicle types, so as to obtain reliable and accurate emission measurements. Kousoulidou et al. (2013) used PEMS to collect emissions from both gasoline and diesel vehicles, and validate the corresponding emission factors in COPERT model (COmputer Programme to calculate Emissions from Road Transport). Unfortunately, the majority of these existing studies failed to form an integrated monitoring system to collect carbon emissions and the related factors simultaneously.

For investigations on traffic-related carbon emissions, the majority of existing studies have focused on the principle of carbon emissions within fixed time-space scale.

At microscopic level, recent studies mainly focused on revealing the relationship between carbon emissions and driving characteristics based on second-by-second data. Abou-Senna and Radwan (2013) used VISSIM (Verkehr In Städten-SIMulationsmodell in German) and MOVES (MOtor Vehicle Emission Simulator) to investigate the effect of major parameters on CO_2 emissions. The results indicate that speed generally has significant impact on CO_2 emissions when the detailed microscopic vehicular operations of acceleration and deceleration are considered. Initially developed by Jimenez (1998), vehicle specific power (VSP) is reported as the instantaneous power per unit mass of the vehicle. The definition has then been used in activity-based modes and to quantify emission variation of various operational states, including idle, acceleration, cruise, and deceleration (Coelho et al., 2009). Ritner et al. (2013) accounted for acceleration and deceleration carbon emissions in urban intersections, and found that acceleration emissions were in an order of magnitude larger than cruise emissions, while deceleration emissions are smaller than cruise emissions. Furthermore, Song et al. (2013) proved that VSP distribution is an effective explanatory parameter of carbon emissions.

At mesoscopic level, various emission models were proposed to evaluate the carbon emissions on road networks (Kota et al., 2012). The models were mainly divided into two groups. Driving cycle based models, such as MOBILE and EMFAC (EMission FACtors), rely mainly on speed distribution, while operating mode based models, including IVE (International Vehicle Emission) and MOVES, depend on VSP distribution. In the United States, the existing official model of Environmental Protection Agency (EPA) for estimating vehicular emissions is MOVES, which quantifies emission as a function of the vehicular operating mode. Fujita et al. (2012) conducted an on-road mobile source emission survey, and then compared to MOVES2010, MOBILE6.2 and EMFAC2007. An overall increase in motor vehicle nonmethane hydrocarbon (NMHC) emissions was identified during hot days that are not fully accounted for by the emission models. Moreover, the ability of EPA's MOVES model to simulate varying vehicle operating modes places increased importance on the choice of operating modes to evaluate project-level emissions. Liu et al. (2013) used MOVES for emission factor estimation and concluded that the regional vehicle operating characteristics should be considered.

At macroscopic level, emission models are usually used for large-scale analysis, aiming to estimate the total amount of emission and establish regional emission inventories. Although models e.g. MOBILE, COPERT and IVE are widely used, they are unfortunately designed to quantify emissions in United States or European countries. Meanwhile, empirical models provided in the previous research mainly focused on the particularly study areas. When applied in other areas, different vehicular operating conditions and emission performances may lead to significant biases. Despite the above models, Inter-governmental Panel on Climate Change (IPCC) offered two emission quantification models at macroscopic level, namely the top-down model and the bottom-up model (Eicker et al., 2008). Both models were used to set up traffic-related emission inventories in seven Chilean cities, analyzing the applicable condition of each model, respectively (Eicker et al., 2008). It was found that the top-down model calculates the total carbon emission amount based on fuel consumption, which has rather high accuracy but is unable to quantify subdivision carbon emission. On the contrary, the bottom-up model calculates carbon emissions based on vehicle-mile of travel (VMT), which is able to quantify subdivision carbon emission and the computational accuracy depends on a variety of emission factors.

The purpose of this study is to propose a comprehensive mobile monitoring model and calculate carbon emissions at microscopic, mesoscopic and macroscopic levels, respectively based on the mobile monitoring data. The remainder of the paper is organized as follows. Section 2 constructs a carbon monitoring system to collect vehicular emissions, as well as the related traffic flow, meteorological conditions and driving characteristics. Then, Section 3 investigated traffic carbon emissions from hierarchical aspects, including microscopic, mesoscopic and macroscopic levels, thus to ascertain the principle relationship with different vehicular operation parameters, travel conditions for particular road or segment, and the overall road transportation system. Finally, conclusions and recommendations for future work are provided in Section 4.

2. Experiment design and data collection

To collect carbon emissions and the related factors under different conditions, traffic carbon emission mobile monitoring system (TCEMMS) based on on-board emission measurement was proposed. Field monitoring was then carried out to provide sufficient data for identifying meaningful factors, calibrating the emission model and quantifying regional-level emissions.

2.1. Mobile monitoring system

As presented in Fig. 1, TCEMMS system was mainly composed of three components. Carbon emission and driving characteristics monitoring module (CEDCM) is the core, mainly collecting second-by-second carbon emissions and driving characteristics of the experimental cars based on PEMS equipment. Traffic information and road conditions collecting module (TIRCCM) acquires traffic flow information and road conditions based on radar speed detector and video camera. Meteorology monitoring module (MMM) mainly collects temperature, humidity and air pressure data.

2.2. Field measurement

The monitoring experiment was carried out along fixed routes using cycle test method at two chosen experiment areas on 25th and 26th November 2014, lasting for 6 h in total. Both off-peak (15:00–16:00) and peak hours (17:00–18:00) were included during the monitoring. Skoda Superb (manufactured in 2010, 2.0 L displacement) and Buick Regal (manufactured in 2013, 2.0 L displacement), the passenger cars with the largest quantity of ownership in Shanghai, were chosen as the experimental vehicles. A total of 12,740 carbon emission and driving characteristics datasets, 2548 meteorology datasets and 16,239 traffic flow datasets were collected.

As presented in Fig. 2, the testing routes were carefully designed to contain various types of road facilities, considering road grade, traffic volume, extent of traffic congestion and temporal traffic flow distribution (Hu et al., 2012; Sun and Elefteriadou, 2012). Fig. 2(a) presents the first testing route, locating at Minhang district, a suburb area in Shanghai. With a total length of 11.5 km, the experimental route contains two east-west and five south-north roads, classified into arterial, secondary arterial and branch. Fig. 2(b) presents the second testing route along Gushan section, S19 expressway, Wuxi, with a total length around 4 km.

The related equipment utilized during the monitoring experiment was presented in Table 1. Real-time vehicular driving data were obtained from the On-Board Diagnostic module of PEMS equipment OBEAS-3000, by inserting the probe sensor directly into the exhaust pipe of the experimental vehicle. Four wide-coverage video cameras were installed on the car to capture traffic states from different view angles (right, left, front and backward), from which the necessary traffic related parameters (traffic volume, vehicle type distribution, and the number of lanes) were obtained through image recognition and information processing. Additionally, velocities of the traffic flow were obtained from radar speed detectors. A meteorology monitor was set along the roadside at 1.5 m above the ground to obtain meteorological condition synchronously.

3. Result analyses and discussion

This section analyzed traffic carbon emissions from different aspects, including microscopic, mesoscopic and macroscopic aspects, thus to investigate the principle relationship with different vehicular operating parameters, travel conditions for particular road or segment, and the overall road transportation system, respectively.

3.1. Microscopic level study

Studies on microscopic traffic-related carbon emission generally aim at analyzing the changing rules of carbon emission rates with driving states, so as to investigate the correlation between carbon emissions and the driving parameters. The corresponding results may provide guidelines for emission model selection at mesoscopic level.

Apart from vehicular emission characteristics, such as engine displacement and emission standard, carbon emissions at microscopic level are mainly affected by driving characteristics, such as velocity, acceleration, engine speed and VSP (Wang et al., 2008b). In addition to the four driving characteristic parameters, CO, CO_2 and HC were chosen as representative carbon emissions. Calculation of VSP is presented in Eq. (1).

$$\mathrm{VSP} = v \times (1.1 \times a + 0.132) + 0.000302 \times v^3 \tag{1}$$

where,

v is the instantaneous velocity of vehicle, m/s; and
a is the instantaneous acceleration of vehicle, m/s^2.

Due to the vibration caused by road roughness, PEMS equipment only collected second-by-second driving characteristics and emissions instead of providing continues data. Linear interpolation was introduced to fill in the missing data between seconds and to replace the identified outliers. Then, carbon emissions and the four parameters

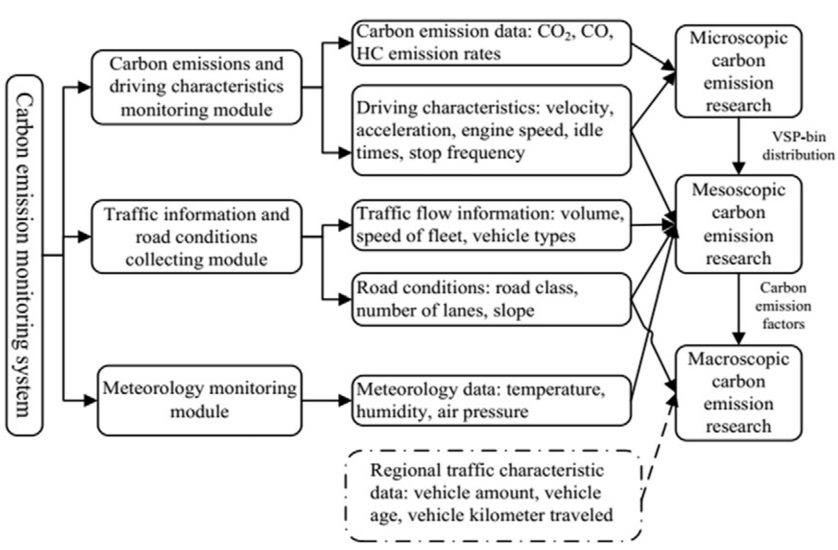

Fig. 1. Architecture of traffic carbon emission mobile monitoring system.

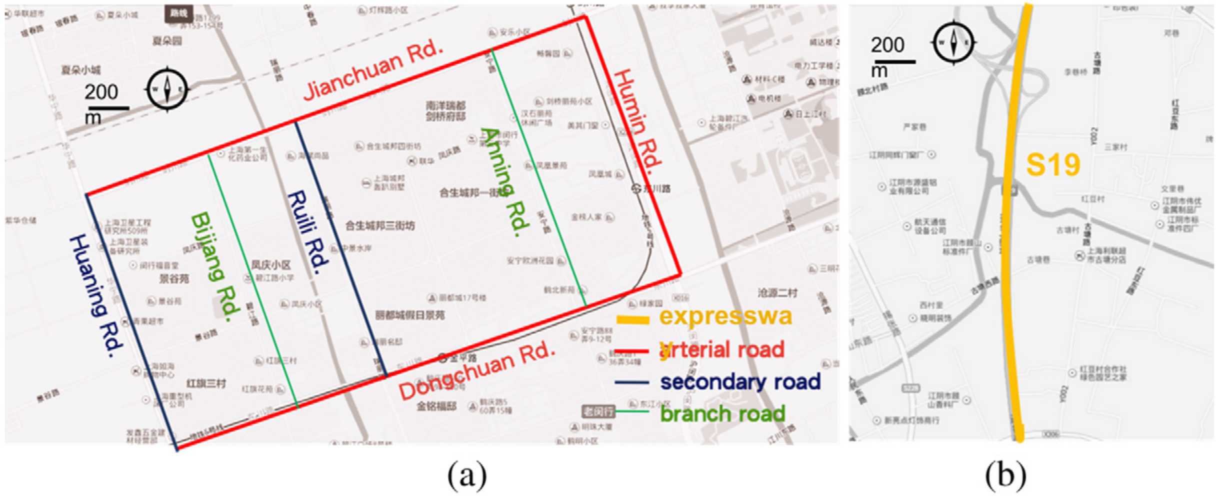

Fig. 2. Carbon emission monitoring areas; (a) road network in Minhang District, Shanghai; (b) Gushan section of S19 Expressway, Wuxi, China.

(velocity, acceleration, engine speed, and VSP) were aggregated into small intervals.

Fluctuations of carbon emission with driving characteristics were presented in Fig. 3(a)–(d). It was found that carbon emissions were generally positive correlated with the driving parameters. Particularly, CO and CO_2 emission rates change almost proportionally with the engine speed and VSP.

Notably, the dynamic variation of carbon emission is time-dependent during the idling condition. As presented in Fig. 4, carbon emissions went through a process from high to low and then smoothed gradually after the vehicle stopped. CO and HC emissions reached the steady states after 20 s, while CO_2 emission attained a steady state 5 s later. The time variation characteristics of carbon emissions during idling condition should also be considered within the emission model.

To quantify the correlation, Pearson correlation coefficient was introduced as calculated in Eq. (2), with the results presented in Table 2.

$$r_{xy} = \frac{\sum(x-\overline{x})(y-\overline{y})}{(n-1)S_x S_y} \tag{2}$$

where:

r_{xy} is the Pearson correlation coefficient;
x is the driving characteristic parameter, including Velocity, Acceleration, VSP and Engine Speed;
$\overline{x}$ is the average of driving characteristic parameter;
y is the carbon emission, including CO, HC, and CO_2;
$\overline{y}$ is the average of carbon emission;
n is the sample size;
S_x is the standard deviation of driving characteristic;
S_y is the standard deviation of carbon emission.

As can be figured out, all coefficients are positive, indicating the definite positive correlation between the carbon emissions and driving characteristics. Compared with CO and CO_2, HC emission is weakly correlated with driving characteristics, which may be explained as the exhaustion of HC is a rather complicated process. Apart from tailpipe, HC emission may also be generated from crankcase exhaustion, fuel leak and evaporation, whereas PEMS equipment limits to tailpipe exhaust data collection only. Consequently, it is difficult to obtain accurate amount of HC emission based on PEMS. An additional model is required to calculate the emission factor of HC, by capturing the effects of each individual HC emission process, such as exhaustion, leak and evaporation.

Among the four parameters, engine speed has the highest correlation, followed by VSP, velocity and acceleration in a descending order. The further Granger causality test results suggested that at 95% confidence level, engine speed had significant causal relationship with CO, HC and CO_2 emissions, while VSP merely had significant causal relationship with CO and HC emissions. As a result, engine speed was identified as the primary factor influencing carbon emissions at microscopic level. However, considering the scarcity of engine speed based models, VSP was finally chosen as benchmark and used on the basis of the common VSP based emission models to achieve high accuracy and performance in calculating the carbon emission factors.

3.2. Mesoscopic level study: carbon emission and road type

Taking the network traffic flow as the research subject, studies on mesoscopic traffic-related carbon emission generally aims at identifying the impacts of traffic flow states and other factors, such as road and meteorological conditions.

Table 1
Traffic carbon emission mobile monitoring equipment.

Equipment	Model	Usage	Detailed parameters
Portable emissions Measurement system	OBEAS-3000	Carbon emissions and driving characteristics collection	Carbon emission: ELD exhaust analyzer; Driving characteristics: on-board diagnostics; Analysis module: master control PC; Sensor: NDIR infrared sensor, electro-chemical sensor
Radar speed detector	Bushnell 10-1921	Speed monitoring	Velocity range: 0.1–321 km/h; Measuring range: 0–456 m; Accuracy: ±1 km/h
Weather & environmental meter	Kestrel NK4500	Meteorology monitoring	Temperature: −29–70 °C Humidity: 0–100% Air pressure: 300–1100 hPa/mb

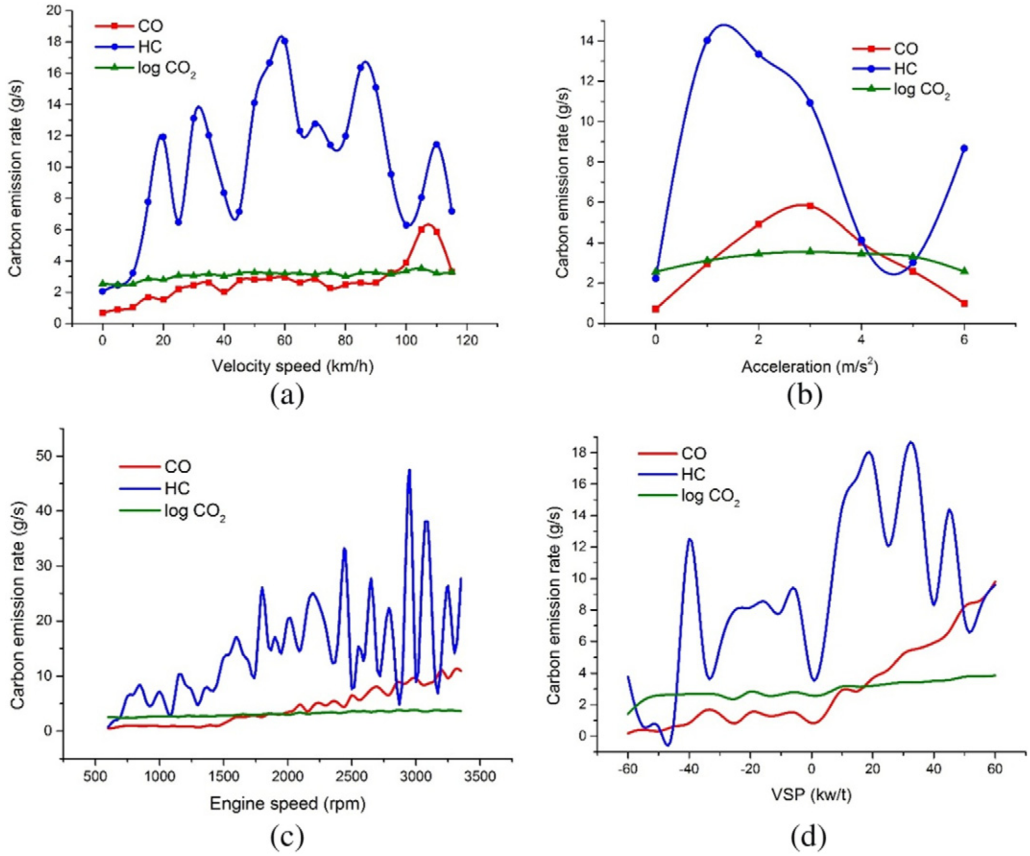

Fig. 3. Changes of vehicular carbon emission with driving characteristics; (a) velocity-emission; (b) acceleration-emission; (c) engine speed-emission; (d) VSP-emission.

3.2.1. Distribution of VSP-bin

According to the microscopic level study, carbon emissions correlate closely with VSP. In other words, the distribution of VSP reflects the temporal and spatial changing patterns of carbon emissions. Therefore, the VSP-based emission model MOVES was chosen to calculate carbon emission factors, so as to describe vehicle state based on VSP-bin distribution. Road condition, meteorological information and traffic flow were also considered, in which the major meteorological information used are temperature and humidity, both largely affecting the evaporative emission process (Abou-Senna and Radwan, 2013). The calculation principle of MOVES model is presented in Eq. (3).

$$TE_{p \cdot st} = \left(\sum ER_{p,bin} \times Ac_{bin}\right) \times Aj_p \tag{3}$$

where,

TE is the carbon emission factor;
p is the emission process;
st is the source type;
ER is the emission rate;
bin is the operation mode segment;
Ac is the driving characteristics;
Aj is the adjust factor of emission.

Since VSP was calculated from second-by-second velocity and acceleration data, four sections were categorized as idle (<2 km/h), low velocity (2 km/h, 40 km/h), medium velocity (40 km/h, 80 km/h) and high velocity (≥80 km/h), each containing several VSP-bin segments. The proportion of each VSP-bin on different road categories was then figured out. Fig. 5 presents the speed-specific distribution of VSP-bin on different road types. As shown in Fig. 5, VSP distributes differently across road types because of the influences of traffic volume, signal control and speed limit. The proportion of idle mode is much higher on arterials. On secondary roads and branches, VSP values are distributed mainly in low-speed section, while most VSP values are in the high-speed section on expressways.

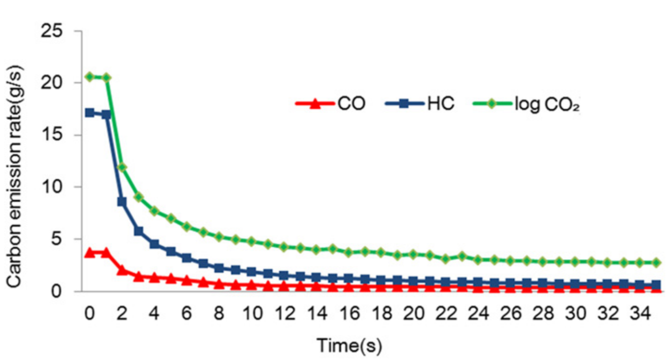

Fig. 4. Changes of vehicular carbon emission during idling condition.

3.2.2. Carbon emission factors

The operating mode data was then incorporated into MOVES model and a project-level analysis was conducted along with the information obtained from the monitoring system. Parameter calibration was carried out to localize MOVES model and improve the accuracy of the

Table 2
Correlations between carbon emissions and vehicular operation parameters.

Parameter	CO (g/s)	HC (g/s)	CO_2 (g/s)
Velocity (km/h)	0.805	0.369	0.793
Acceleration (m/s^2)	0.77	0.492	0.86
VSP (kw/t)	0.913	0.609	0.847
Engine speed (rpm)	0.959	0.64	0.902

emission factors. According to Motor Gasoline National Standards (GB17930-2013), fuel type that matches Chinese standards within the fuel database was chosen. Age distribution of vehicles and I/M (Inspect/Maintenance) information were obtained from the local I/M station. Moreover, various emission processes, such as fuel evaporation and crankcase exhaustion were incorporated to calculate the emission factors accurately.

For comparison purpose, PEMS data were introduced to calculate the emission factors, by using the amount of Carbon emissions divided by travel distance. Carbon emission factors calculated by MOVES and PEMS data are presented in Table 3. Taking the various emission processes into consideration, emission factors calculated by MOVES are slightly higher than those by PEMS data. The phenomenon can be explained that in MOVES model, fuel evaporation and crankcase exhaustion were incorporated to calculate the emission factors, while PEMS data only contains tailpipe exhaust.

To verify the reliability of MOVES model, Cronbach α coefficient was calculated to check the consistency of the two models, as shown in Eq. (4).

$$\alpha = \frac{n}{n-1}\left(1-\frac{\sum_{i=1}^{n} S_i^2}{S_T^2}\right) \tag{4}$$

where,

α is the reliability coefficient, $\alpha \in [0, 1]$;
n is the number of roads;
S_i^2 is the interclass variance of MOVES set and PEMS set;
S_T^2 is the population variance.

If $\alpha > 0.9$, data consistency is excellent; if $0.8 \le \alpha \le 0.9$, data consistency is acceptable; $0.7 \le \alpha < 0.8$ indicates the emission factors need to be modified; if $\alpha < 0.7$, the emission factors are unreliable (Nunnally and Bernstein, 1994). The Cronbach α reliability coefficients of CO_2, CO, HC were calculated as 0.82, 0.95 and 0.93, respectively, indicating that the emission factors from calibrated MOVES model are reliable in developing carbon emission inventory at macroscopic level.

3.2.3. Influence of road type

According to MOVES model, carbon emission factors for different types of roads were calculated and are presented in Table 4. The results along with those from Fig. 5 and Table 3 demonstrated the rather large differences among road types, both for VSP distribution and carbon

Table 3
Carbon emission factors calculated by MOVES model and PEMS data.

Road name	Type	CO_2 (g/km)		CO (g/km)		HC (g/km)	
		MOVES	PEMS	MOVES	PEMS	MOVES	PEMS
S19	Expressway	198.62	192.28	1.22	1.06	0.03	0.03
Humin rd	Arterial	206.03	204.32	1.65	1.63	0.04	0.04
Jianchuan rd	Arterial	321.27	318.34	2.78	2.1	0.12	0.09
Dongchuan rd	Arterial	368.53	363.48	3.64	3.19	0.13	0.1
Huaning rd	Secondary	188.44	183.29	2.01	1.84	0.04	0.03
Ruili rd	Secondary	176.52	171.71	2.71	2.28	0.03	0.02
Anning rd	Branch	173.63	169.63	1.95	1.6	0.03	0.03
Bijiang rd	Branch	270.71	241.55	2.67	1.98	0.05	0.04

emission factors. Therefore, the effects of road type on carbon emissions should be further investigated.

As traffic volume and average speed are important for road classification, the two parameters were selected to represent road type. Carbon emission factors at different levels were then calculated, while sensitivity coefficient SAF, as calculated in Eq. (5), was used for sensitivity analysis.

$$\mathrm{SAF} = \left|\frac{(A_i - A_{i-1})F_{i-1}}{(F_i - F_{i-1})A_{i-1}}\right| \tag{5}$$

where,

A is the carbon emission factor, g/km;
F is the VSP value, kw/t.

Fig. 6 presents the results of sensitivity analysis. If SAF > 1, carbon emission factor is sensitive to the parameter; if $0.1 \le \mathrm{SAF} \le 1$, the parameter is an ordinary sensitive one; otherwise (SAF < 0.1) the parameter is less sensitive. As presented in Fig. 6, it was identified that speed and traffic volume are sensitivity parameters when speed is lower than 80 km/h and traffic volume is lower than 4500 veh/h. In other words, changes of speed and traffic volume significantly influence the carbon emission factors. Consequently, road type should be considered and appropriate emission factors should be chosen during macroscopic studies.

3.3. Macroscopic level study: modified IPCC model

At macroscopic level, vehicular carbon emissions are mainly affected by annual vehicle kilometers travelled (AVKT) and regional vehicle ownership. Studies at macroscopic level generally aim at analyzing the

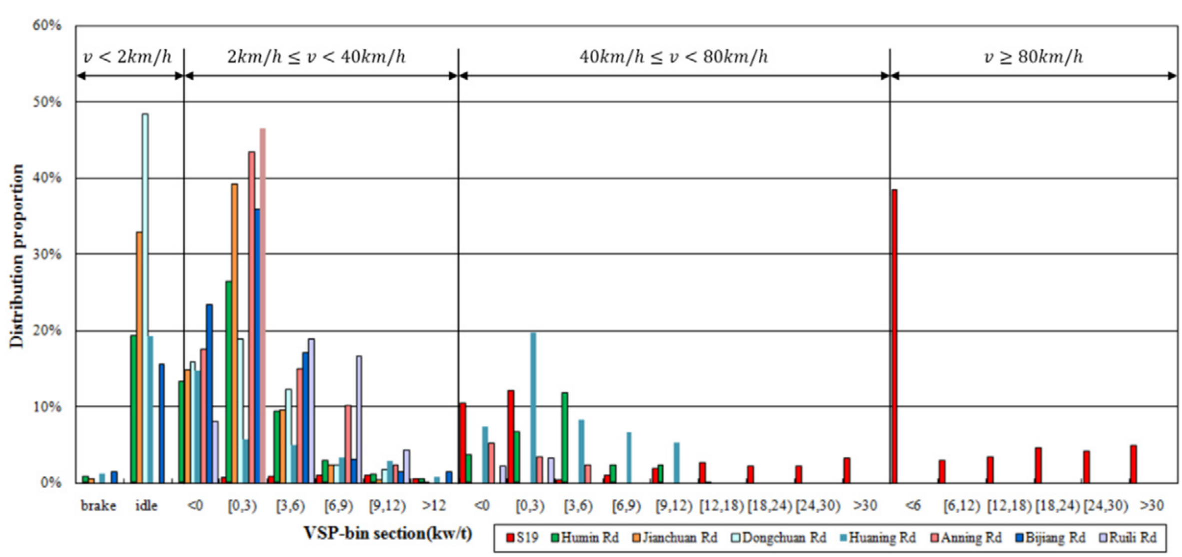

Fig. 5. Distribution of VSP-bin section in each segment.

Table 4
Carbon emission factors on different road type.

Road type	CO_2/(g/km)	CO/(g/km)	HC/(g/km)
Expressway	198.62	1.22	0.03
Arterial road	298.61	2.69	0.1
Secondary road	182.48	2.36	0.04
Branch road	222.17	2.31	0.04

situation of traffic-related carbon emissions and quantifying the annual traffic-related carbon emission amount.

Findings of mesoscopic study indicate that road types largely influence carbon emission factors. Hence, the macroscopic study improves the IPCC bottom-up model based on the influence of road type. The modified model is presented in Eqs. (6)–(8), where vehicle age distribution and accumulating mileage data were obtained from the local I/M station.

$$T_i = \frac{1}{1000}\sum_j S \cdot C \cdot P_j \cdot E_{ij} \tag{6}$$

$$C = \sum_{i=1}^{n} (M_i - M_{i-1}) Q_i \tag{7}$$

$$M = 2.52a^{0.86}\left(R^2 = 0.64\right) \tag{8}$$

where,

T_i is the amount of carbon emission i, kg;
S is the amount of passenger cars, veh;
C is the annual average vehicle kilometers travelled, km;
P_j is the percentage of vehicle travelled distance on road of grade j;
E_{ij} is the emission factor of carbon emission i on road of grade j;
M is the vehicle accumulating mileage, km;
Q is the proportion of vehicle age distribution;
a is the vehicle age.

Taking Shanghai, China as a case study, the proposed model was implemented to obtain the quantitative evaluation of carbon emissions in 2014, as shown in Table 5. The ownership of passenger cars in Shanghai is about 1.83 million, and the annual average vehicle kilometers travelled is 18.6 thousand. The percentage of travelled distance on each type of roads was approximated by referring to the evaluation index system of urban traffic congestion (DB 11/T 785-2011).

From the quantitative evaluation, arterials were found as the major carbon emission source among the urban road system, accounting for over 50% carbon emissions with only about 41% total vehicular travelled distance. Carbon emission arises largely from excessive traffic flow on the arterial roads. According to the traffic flow monitoring, arterial roads share the main traffic volume in urban area, suffering from severe congestion during the rush hours. Associated with the studies at microscopic and mesoscopic levels, vehicular operating modes on arterial roads were distributed mainly in idle and low-speed section, which generally induces the poor fuel economy and excessive carbon emissions. Therefore, an important task of promoting low-carbon transportation is to reduce the arterial carbon emissions.

Table 5
Carbon emission situations at macroscopic level.

Road type	Distance travel	Carbon emissions (kt)				Contribution rate
		CO_2	CO	HC	Total	
Expressway	20%	1355.3	8.32	0.21	1363.83	16.32%
Arterial road	41%	4177.1	37.63	1.41	4216.14	50.49%
Secondary road	16%	996.1	12.88	0.22	1009.2	12.09%
Branch	23%	1743.4	18.12	0.31	1761.83	21.1%
Overall	100%	8271.9	76.95	2.15	8350.99	100%

4. Conclusions and recommendations

This study constructed a comprehensive and efficient tool to collect traffic-related carbon emission data using mobile monitoring system, consisting of PEMS and a variety of environmental meters. Then, by taking typical road networks as experimental areas, carbon emissions and the corresponding impact factors were collected, so that traffic-related carbon emissions were analyzed at different temporal-spatial scales. At microscopic level, correlation between carbon emissions and driving characteristics was investigated using the second-by-second data. It was found that the rising trends in VSP and engine speed have a significant positive correlation with carbon emissions. At mesoscopic level, road network and traffic flow were studied and the VSP-based emission model MOVES was utilized to calculate emission factors based on the results from microscopic level. Sensitivity analyses were performed to verify the effect of road type on carbon emission. At macroscopic level, the study improves the IPCC bottom-up model by taking road type into consideration and quantifies the overall traffic-related carbon emission amount in Shanghai, 2014. The quantitative results identify that arterial traffic was the major source to carbon emissions in urban road transportation. The results connected traffic-related carbon emissions from microscopic to macroscopic levels, putting forward a perspective to quantify regional carbon emissions using second-by-second data.

Although the results are promising, future studies could be conducted to improve the performance and practicability of the emission model. According to the study at microscopic level, engine speed has the highest correlation with carbon emissions, indicating the development of engine speed-based emission model may achieve higher accuracy. Moreover, since the arterials are the major carbon emission source, emission reduction strategies may be developed from two aspects: 1) To channel the traffic flow by low-carbon oriented guidance, so as to

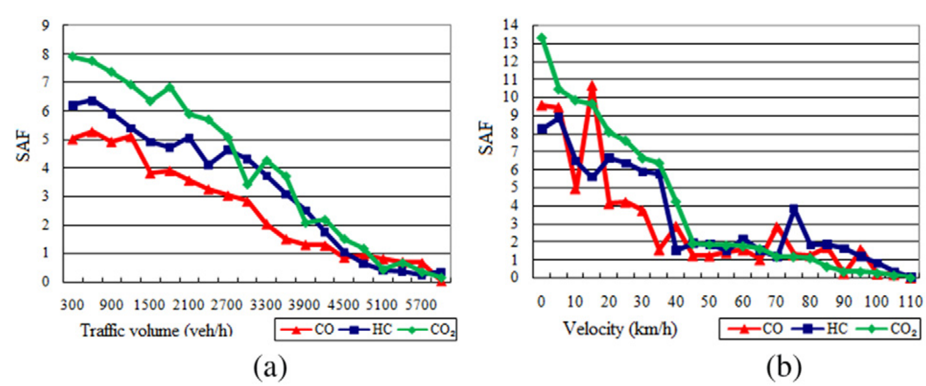

Fig. 6. Sensitivities of emission factors with velocity and traffic volume; (a) traffic volume-SAF; (b) velocity-SAF.

alleviate the carbon-related emissions on urban arterials; or 2) To incorporate the objective of low-carbon emission into signal coordination control, so as to reduce the carbon emissions caused by frequent acceleration and idling.

Acknowledgements

The authors would like to express their appreciation to Drs. Zhong-Ren Peng, Qingchang Lu and Yi Zhu from School of Naval Architecture Ocean and Civil Engineering, Shanghai Jiao Tong University for their valuable suggestions and assistance in this study. The research was supported in part by the Humanities and Social Science Research Project [15YJCZH148], Ministry of Education, China, the Philosophy and Social Science Research Project of Shanghai [2014BGL009], China, and the Research Foundation from Center for Urban Development and Land Policy, Peking University – Lincoln Institute [FS05-20161101-SJ]. Any opinions, findings and conclusions or recommendations expressed in this paper are those of the authors and do not necessarily reflect the views of the sponsors.

References

Abou-Senna, H., Radwan, E., 2013. VISSIM/MOVES integration to investigate the effect of major key parameters on CO_2 emissions. Transp. Res. D 21, 39–46.
Aleklett, K., Höök, M., Jakobsson, K., 2010. The peak of the oil age: analyzing the world oil production reference scenario in world energy outlook 2008. Energ Policy 38 (3), 1398–1414.
Burns, K., Skally, M., Solomon, K., Scott, L., Mcdermott, S., OFlanagan, D., 2012. Estimating mobile-source greenhouse gas emissions in Los Angeles County, California. Transportation Research Record: Journal of the Transportation Research Board, 2303. Transportation Research Board of the National Academies, Washington, D.C., pp. 61–70.
Coelho, M.C., Frey, H.C., Rouphail, N.M., 2009. Assessing methods for comparing emissions from gasoline and diesel light-duty vehicles based on microscale measurements. Transp. Res. D 14 (2), 91–99.
DeFries, T.H., Sabisch, M., Kishan, S., 2014. In-use fuel economy and CO_2 emissions measurement using OBD data on US light-duty vehicles. SAE Int. J. Engines 7 (3), 1382–1396.
Eicker, M.O., Zah, R., Triviño, R., 2008. Spatial accuracy of a simplified disaggregation method for traffic emissions applied in seven mid-sized Chilean cities. Atmos. Environ. 42 (7), 1491–1502.
Franco, V., Kousoulidou, M., Muntean, M., 2013. Road vehicle emission factors development: a review. Atmos. Environ. 70, 84–97.
Fujita, E.M., Campbell, D.E., Zielinska, B., 2012. Comparison of the MOVES 2010a, MOBILE 6.2, and EMFAC 2007 mobile source emission models with on-road traffic tunnel and remote sensing measurements. J. Air Waste Manage. Assoc. 62 (10), 1134–1149.
Guo, H., Zhang, Q.Y., Shi, Y., 2007a. Evaluation of the International Vehicle Emission (IVE) model with on-road remote sensing measurements. J. Environ. Sci. 19 (7), 818–826.
Guo, H., Zhang, Q.Y., Shi, Y., 2007b. On-road remote sensing measurements and fuel-based motor vehicle emission inventory in Hangzhou, China. Atmos. Environ. 41 (14), 3095–3107.
Hu, J., Wu, Y., Wang, Z., 2012. Real-world fuel efficiency and exhaust emissions of light-duty diesel vehicles and their correlation with road conditions. J. Environ. Sci. 24 (5), 865–874.
Jimenez, J.L., 1998. Understanding and Quantifying Motor Vehicle Emissions with Vehicle Specific Power and TILDAS Remote-sensing. Massachusetts Institute of Technology (Ph.D. Thesis).
Kota, S.H., Ying, Q., Schade, G.W., 2012. MOVES vs. MOBILE 6.2: differences in emission factors and regional air quality predictions. Paper Presented at the 91st Annual Meeting of the Transportation Research Board, Jan. 2012, Washington, D.C.
Kousoulidou, M., Fontaras, G., Ntziachristos, L., 2013. Use of portable emissions measurement system (PEMS) for the development and validation of passenger car emission factors. Atmos. Environ. 64, 329–338.
Liu, H., He, K., Lents, J.M., 2009. Characteristics of diesel truck emission in China based on portable emissions measurement systems. Environ. Sci. Technol. 43 (24), 9507–9511.
Liu, H., Wang, Y., Chen, X., 2013. Vehicle emission and near-road air quality modelling in Shanghai, China, based on taxi GPS data and MOVES revised emission inventory. Transportation Research Record: Journal of the Transportation Research Board, 2340. Transportation Research Board of the National Academies, Washington, D.C., pp. 38–48.
Nunnally, J.C., Bernstein, I.H., 1994. The assessment of reliability. Psychometric Theory 3 (1), 248–292.
Pelkmans, L., Debal, P., 2006. Comparison of on-road emissions with emissions measured on chassis dynamometer test cycles. Transp. Res. D 11 (4), 233–241.
Ritner, M., Westerlund, K.K., Cooper, C.D., 2013. Accounting for acceleration and deceleration emissions in intersection dispersion modelling using MOVES and CAL3QHC. J. Air Waste Manage. Assoc. 63 (6), 724–736.
Smit, R., Ntziachristos, L., Boulter, P., 2010. Validation of road vehicle and traffic emission models-a review and meta-analysis. Atmos. Environ. 44 (25), 2943–2953.
Song, G., Yu, L., Xu, L., 2013. Comparative analysis of car-following models for emission estimation. Transportation Research Record: Journal of the Transportation Research Board, 2341. Transportation Research Board of the National Academies, Washington, D.C., pp. 12–22.
Sun, D.J., Elefteriadou, L., 2012. Lane-changing behavior on urban streets: an “in-vehicle” field experiment-based study. Comput. Aided Civ. Inf. Eng. 27 (7), 525–542.
Wang, H., Chen, C., Huang, C., 2008a. On-road vehicle emission inventory and its uncertainty analysis for Shanghai, China. Sci. Total Environ. 398 (1), 60–67.
Wang, H., Fu, L., Zhou, Y., 2008b. Modelling of the fuel consumption for passenger cars regarding driving characteristics. Transp. Res. D 13 (7), 479–482.
Zhang, Z., 2011. Assessing China's carbon intensity pledge for 2020: stringency and credibility issues and their implications. Environ. Econ. Policy Stud. 13 (3), 219–235.